Stone columns – group behaviour and influence of footing flexibility

W.C.S. Wehr
Keller Holding GmbH, Offenbach, Germany

ABSTRACT: Recent research on the group action of stone columns points out that the behaviour of an isolated single column is quite different from the one of a stone column in a group of columns under a rigid footing. To highlight the differences, model tests of a rigid footing on a single sand column in clay and model tests of a rigid footing with various numbers of sand columns in clay are compared. Deformations of groups of stone columns depend as well on the rigidity of the footing. In order to demonstrate the different deformation mechanisms, model tests by Hu (1995) with a rigid and a flexible footing are compared.

Additionally a FE-re-calculation of the model tests is performed with an elasto-plastic constitutive model taking into account the mean grain diameter. Beginning with a single isolated column, the deformation mechanism of the column has been reproduced, detecting a wedge shaped shear zone below the footing. The same footing on 20 columns has been analysed to study the group effect. At the end the deformation mechanism of a group of columns below a flexible footing is reproduced. Finally recommendations for practical applications are given.

1 INTRODUCTION

Modelling forces and displacements of stone columns, the width of shear zones has to be considered correctly. This applies for single columns and for groups of columns as well (Wehr 1999a, Wehr 2004). The influences of different parameters like initial density, pressure level and mean grain diameter on the width of the shear zone was studied intensively with model tests (Tejchman '89, Hammad '91, Hassan '95) and could be reproduced with FE-calculations (Tejchman '97, Tejchman et al. '99).

Hu 1995 and Wood/Hu 1997 have observed in model tests with a group of stone columns, that the deformation mechanism depends on the stiffness of the footing.

In this publication model tests on a group of stone columns below a rigid and a flexible footing are compared, before re-calculations of the model tests by means of the finite element method are presented. The aim is to clarify the different deformation mechanisms, but not to curve fit the force displacement curves exactly. The latter is reserved for 3D-calculations.

2 MODEL TESTS

Model tests with groups of sand columns in clay have been executed by Hu ('95) and Wood ('98) to get a closer insight into the deformation mechanisms of a group of stone columns under footings.

The soils of the model tests are Speswhite kaolin clay which was reconstituted from a slurry with a plasticity index of 27 and an average undrained cohesion of c_u = 13 kPa, and a poorly graded medium Loch Aline sand (d_{50} = 0.32 mm, e_{max} = 0.80, e_{min} = 0.56, $0.67 < e < 0.74$).

The preparation of the tests, the set-up and all soil and column parameters used were described in detail by Hu (1995). A summary may be found in Wehr (2004).

2.1 *Stiff footing*

All 16 model tests with columns below a rigid footing were executed using displacement control with a velocity of v = 0,061mm/min. Compared to the tests with single stone columns by Witt (1978) with a ve-

locity of v = 0,5 mm/min and a testing time of only 40 min the eight times smaller velocity in the tests by Hu does not plays a negligible role. Therefore the stiffness of the clay will most likely increase with testing time. The contribution of the loading velocity on the force and settlement of piles have been shown by Krieg et al. (1998).

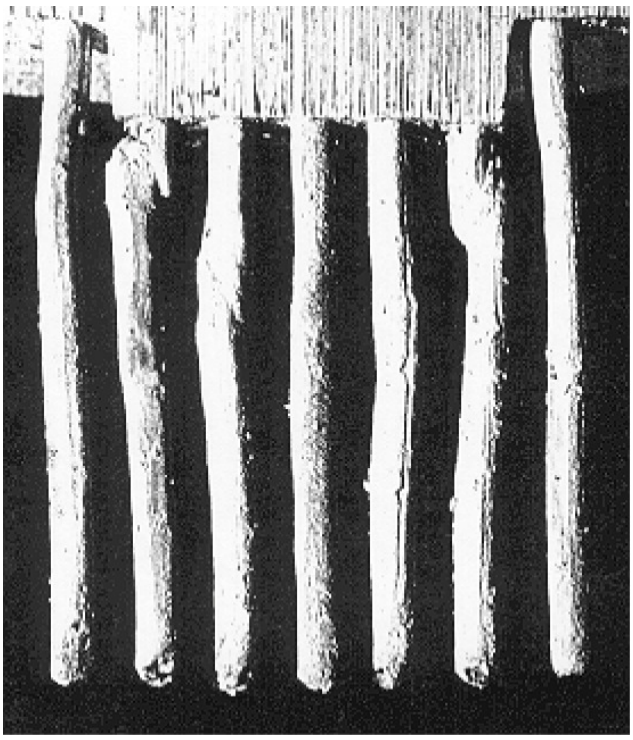

Figure 1. Deformed group of long slender columns, test TS17 (Hu '95)

The main result in terms of deformation under the footing is that a wedge shaped body is displaced vertically in connection with bulging and buckling of the columns, see Fig. 1. Buckling was observed near the edges of the footing close to the ground surface and bulging occurred under the center of the footing in a deeper region. The columns adjacent to the footing showed only a small amount of bending.

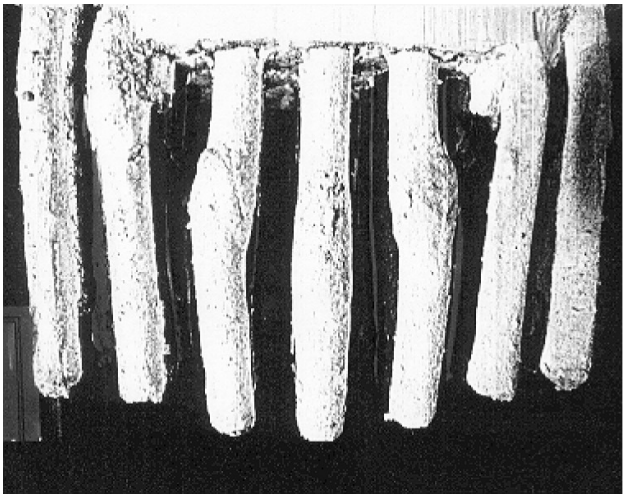

Figure 2. Deformed group of short thick columns, test TS08 (Hu '95)

The load bearing mechanism is significantly influenced by the length of the columns as compared to the diameter of the footing *D*. If the length of the columns *l* is less than or equal to *D* ($l \leq D$), the base of the columns will transfer the load to the underlying clay resulting in a significant punching of the columns, Fig. 2. But if the length of the columns is larger than 1.5*D* the penetration of the columns into the clay is insignificant.
This mechanism could be reproduced by FE-calculations by Wehr (2004). Additionally shear zones in the clay were detected which were not visible in the model tests due to their small thickness.

2.2 *Flexible footing*

Furthermore one test with a flexibel footing has been executed, Hu (1995). The load was applied by a pressurized cylinder with its bottom part being a rubber membrane. The installation of the columns was not changed with respect to the tests with the stiff footing, however a 4mm thick sandy load distribution layer was used on top of the columns.

In contrast to the tests with a rigid footing this test was executed with load control. After rising the load from p = 120 kPa to p = 140 kPa and 8 days loading time the soil displaced rapidly within a few seconds and the test had to be stopped.

Fig. 3 shows the asymmetric deformation of the columns. No distinct wedge-shaped soil body with shear zones could be observed below the footing.
It will be analysed in the following FE-calculations, if this kind of deformations is typical for a flexible footing.

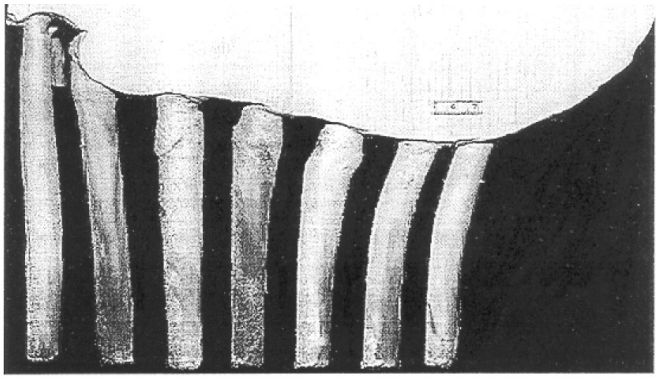

Figure 3. Deformed group of columns below flexible footing (Hu '95)

In Fig. 4 the load displacement curves of different tests with rigid and flexible footing are presented.

Test TS17 of fig.1 and 4 (rigid) with c_u=14kPa, column diameter d_s=11mm and column length l_s=160mm differs from test TS09 (rigid) because of the different column diameter d_s=17.5mm. In Fig. 4 it may be seen, that slightly higher loads are applicable in test TS09.

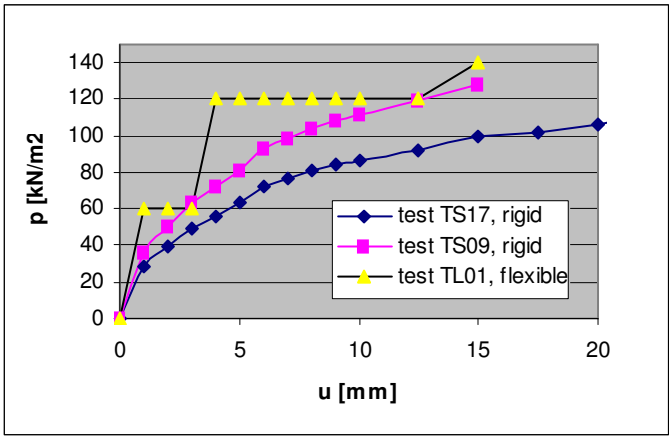

Figure 4. Load-displacement curve below a rigid and flexible footing (after Hu 1995)

Test TL01 (flexible) corresponds to test TS09 (rigid) apart from the slightly higher c_u=18kPa which results again in a higher applicable load, fig. 4. The extraordinary high load steps in this test were leading to failure which can be guessed nearly optically.

3 ELASTO-PLASTIC CONSTITUTIVE LAW

The Cosserat elasto-plastic constitutive model used here includes isotropic hardening and softening. It has been proposed by Mühlhaus ('87) and is described in detail by Tejchman ('89,'97) and Tejchman/Wu ('93) and Wehr ('99).
Differences from the conventional theory of plasticity are the presence of Cosserat rotations and couple stresses using the mean grain diameter as a characteristic length.

In Table 1, the parameters of the elasto-plastic model for the two materials considered in recalculations of model tests are summarized. The parameters for Karlsruhe sand have been determined by Tejchman ('97) and the parameters for Ahrtal clay has been estimated from the material parameters given by Witt ('78). Modification were necessary due to the loose state only for the peak friction angle and for the E-modulus similar to the parameters by Tejchman (1997). The parameters of Speswhite kaolin clay were estimated from the parameters of test TS17 given by Hu (1995). An important parameter is the cohesion which was determined from vane shear tests. The E-modulus was evaluated using a graph by Ladd et al. (1977) with E/c_u ~100. The Cosserat-constants were not modified compared to Wehr (2004). Their influence have been demonstrated by Tejchman/Wu (1993).

Twelve material parameters are needed to characterise a soil material:

- cohesion c,
- friction angle at peak φ_p and in the critical state φ_c,
- angle of dilatancy $\beta = \beta_1 (\sin\varphi - \sin\varphi_c)$
- modulus of elasticity E,
- Poisson's ratio ν,
- shear strains at the peak γ_p and at the beginning of shearing γ_0
- mean grain diameter d_{50} and
- three Cosserat-constants a_1 to a_3.

Table 1. Material parameters for the elasto-plastic model (Loch Aline Sand, Speswhite clay)

	C	φ_p	φ_c	β_1
	[kPa]	[Grad]	[Grad]	[--]
sand	0	37	35	3
clay	14	0	0	0
	E	ν	γ_p	γ_0
	[MPa]	[--]	[--]	[--]
sand	15	0.3	0.05	0.03
clay	1.4	0.45	0.05	0.03
	d_{50}	a_1	a_2	a_3
	[mm]	[--]	[--]	[--]
sand	0.32	0.375	0.125	1.00
clay	0.002	0.375	0.125	0.25

4 CALCULATIONS

The aim of the next sections is to demonstrate the different deformation mechanisms of a rigid and a flexible footing resting on a soft soil with stone columns. In order to compare both cases the dimensions and soil parameters of the rigid footing has been used for the flexible footing as well.

Utilizing the symmetry of the system only 3.5 of 22 columns have been modelled.

4.1 *Stiff footing*

Fig. 5 shows the upper part of the deformed group of columns after a displacement u=20mm. If these results are compared with Fig. 1, a wedge shaped part of the soil below the footing nearly undergoes no deformation. The edge of this wedge consists of a shear zone partly in the sand columns and partly in the clay having the same inclination in the model test and the calculation. Different deformations are observed in the center column which bulges, and in the middle and outer column where a shear zone (buckling) is observed. This corresponds exactly to the observations made during the model tests by Hu '95.

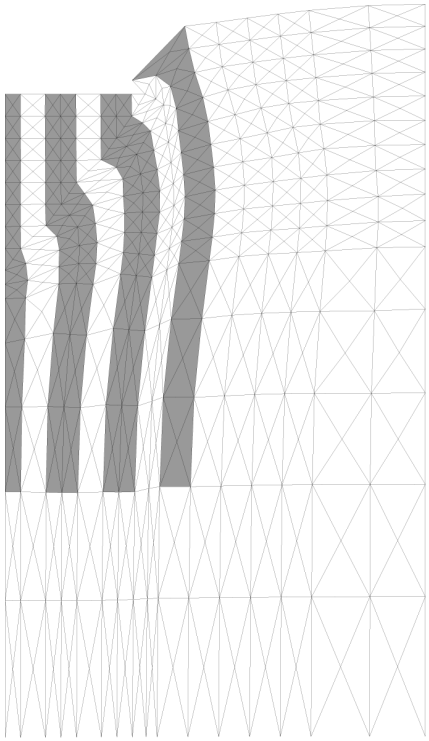

Figure 5. Deformed group of columns below rigid footing, upper part, u=20mm, clay (white) and column (grey)

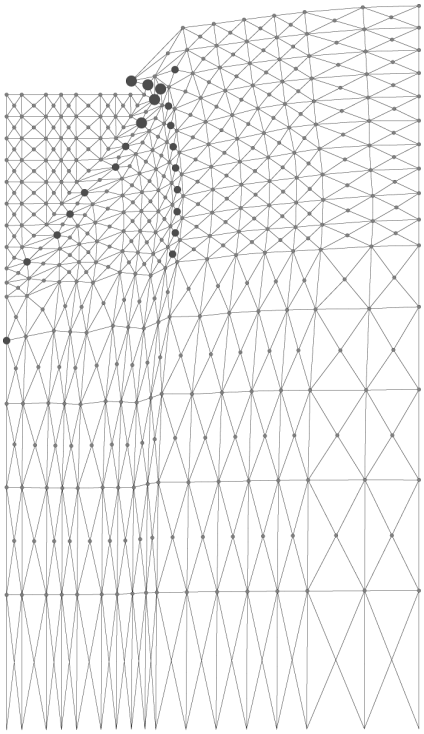

Figure 6. Deformed group of columns below rigid footing, upper part, u=20mm, Cosserat rotations: small circle ω_c = 0.0, large circle ω_c = 3.4

The calculated width of the shear zone around the wedge shaped area in fig.6 is d_s = 4mm ($10d_{50}$). A shear zone in the clay which could not be observed in the model tests due to the small thickness can be detected in fig. 6 near the column at the edge. It is worth to note that this shear zone extends only to a certain depth depending on the displacement of the column relative to the clay.

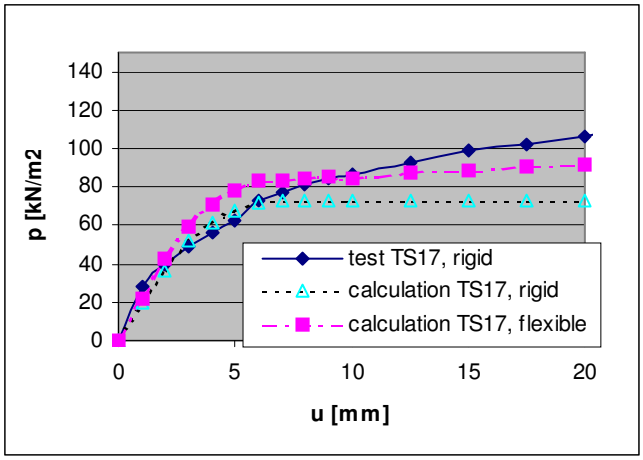

Figure 7. Load-displacement curves of rigid and flexible footing

Fig. 7 shows the load-displacement curves of test TS17 and the recalculation for a rigid footing. Until a displacement of approximately 6mm both curves are rather similar. However for larger displacements there seems to be a growing influence of the consolidation of the clay which has not been taken into account in this model.

4.2 *Flexible footing*

The displacements for a rigid and a flexible footing are chosen equally in a characteristic point which is 0.74**D*/2 apart from the center of the plate with *D* being the diameter of the footing. After a displacement of *u*=10mm in the center of the footing the displacements are $S_{flex} = S_{rigid} / 0{,}75$. The initial state for the flexible footing is a horizontal area. With increasing displacement the bending of the footing increases as well.

In fig. 8 the upper part of the deformed group of columns can be seen below a flexible footing after a displacement of *u*=20mm. In contrast to fig.5 no wedge shaped zone with shear zones and no buckling of columns is observed, but considerable bulging.

The form of shear zones for a flexible footing in fig.9 is different from the one of a rigid footing in fig.6. Starting with a broad vertical shear zone in the clay at the edge of the footing, several approximately wedge shaped and parallel shear zones are created.
The first one starts at the edge of the footing in the clay, cuts the first sand column and ends in the clay between the columns.
The second one starts in a certain distance from the footing edge in the direction of the footing center and progresses in the shape of a wedge, similar to the rigid footing.

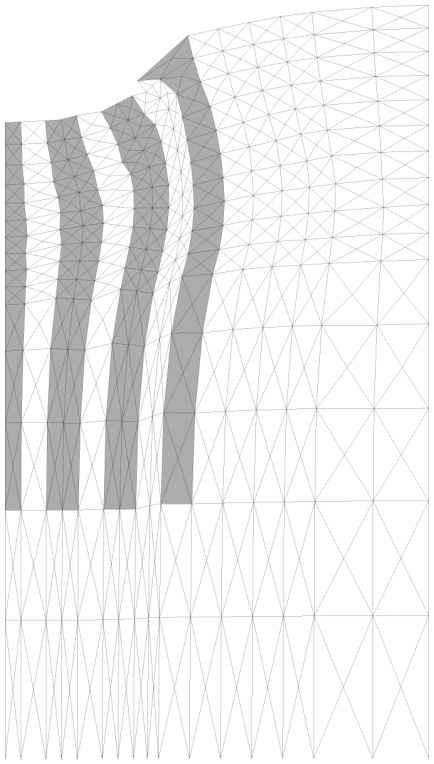

Figure 8. Deformed group of columns below flexible footing, upper part, u=20mm, clay (white) and column (grey)

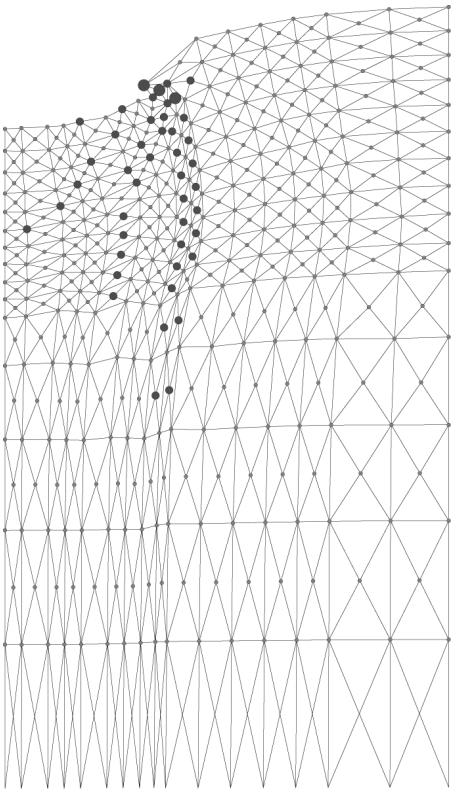

Figure 9. Deformed group of columns below flexible footing, upper part, u=20mm, Cosserat rotations: small circle $\omega_c = 0.0$, large circle $\omega_c = 2.6$

The third one in fig.9 just started at this deformation stage. It starts again further apart from the footing edge and runs parallel to the second one only at deformations larger than 20mm.
Concluding the above a pattern of approximately parallel shear zones is created in the case of a flexible footing. The more shear zones are created, the larger the deflection (bending) of the footing.

Shear zones in the clay which were not observed in the model tests, may be seen in Fig. 9 between all columns and outside the column under the edge of the footing. Note, that these shear zone extends only to a limited depth depending on the movements of the columns relative to the clay. Concerning the widths of the shear zones in clay, they are too large due to too large elements chosen. Between two columns there should exist a shear zone close to each column rather than one shear zone extending from the left column to the right column. The possibility of the unification of two shear zones exists only if two column boundaries are close enough together and the lateral deformation is limited (Wehr '97).

Fig. 7 additionally shows the calculated load-displacement curves of a flexible and a rigid footing. The results may be compared directly, because no other parameter has been changed except of the footing stiffness. The total load which a flexible footing can bear is slightly higher for all deformations than the load of a rigid footing. This is essentially due to the higher forces in the clay which are caused by the wider shear zone below the footing edge and an additional shear zone between the columns.

5 CONCLUSIONS

Model tests of groups of stone columns in clay show a fundamentally different deformation mechanism, if a rigid or a flexible footing is used.
Because of sudden large displacements which occurred during the test with the flexible footing, no general conclusions could be drawn.

Re-calculations of the model tests have been performed by means of the finite element method with an elasto-plastic constitutive law within the Cosserat continuum. In this way, the mean grain diameter which is essential to capture shear zones, is taken into account and the solution is mesh independent.

In the model tests with a rigid footing and in the recalculation a deformation mechanism was observed with a wedge shaped deformation directly below the footing. Buckling was observed near the edges of the footing close to the ground surface and bulging occurred under the center of the footing in a deeper region.

In case of a flexible footing bulging of all columns in the upper part was observed without any buckling of the columns. Cosserat rotations display multiple parallel shear zones forming a shear zone pattern.

The larger the flexibility of the footing, the more shear zones occur.

The applicable load on a flexible footing is always larger than the one on a rigid footing, if the average deformations are equal. It is recommended to construct footings on stone columns only as stiff as necessary making use of the maximum value of the allowable differential settlements.

6 REFERENCES

Hammad, W. (1991): Modelisation non lineaire et etude experimentale des bandes de cisaillement dans les sables. PhD. Thesis, Universite de Grenoble,IMG, Labo 3S

Hassan, A.H. (1995): Etude experimentale et numerique du comportement local et global d'une interface sol granulaire-structure. PhD. Thesis, Universite de Grenoble,IMG, Labo 3S

Hu, W. (1995): Physical modelling of group behaviour of stone column foundations. PhD thesis, University of Glasgow

Krieg S., Goldscheider M. (1988): Bodenviskosität und ihr Einfluß auf das Tragverhalten von Pfählen. Bautechnik, Heft 10, 806-820

Ladd C.C., Foott R., Ishihara K., Schlosser F., Poulos H.G. (1977) Stress-deformation and strength characteristics. State of the art report. Proceedings of the 9th. Int. Conf. on Soil Mech. and Found. Eng., Tokyo,2, 421-494

Mühlhaus H.B. (1987): Berücksichtigung der Inhomogenitäten im Gebirge im Rahmen einer Kontinuumstheorie. Publication of the institute for soil and rock mechanics, Karlsruhe university, vol. 106.

Tejchman J. (1989): Scherzonenbildung und Verspannungseffekte in Granulaten unter Berücksichtigung von Korndrehungen. Publication of the institute for soil and rock mechanics, Karlsruhe university, vol. 117.

Tejchman J. (1997): Modelling of shear localisation and autogeneous dynamic effects in granular bodies. Publication of the institute for soil and rock mechanics, Karlsruhe university, vol. 140.

Tejchman J. (1998): Numerical modelling of shear localisation with a polar hypoplastic approach. 4th Int. Workshop on Localisation and Bifurcation Theory for Soils and Rocks, Gifu, Japan, 323-332

Tejchman J., Wu W. (1993): Numerical study on patterning of shear bands in a Cosserat continuum. Acta Mechanica, Springer Verlag, Vol.99, 61-74

Tejchman J., Herle I., Wehr W. (1999): FE-studies on the influence of initial void ratio, pressure level and mean grain diameter on shear localisation.
Int. Journal for Numerical and Analytical Methods in Geomechanics, Vol. 23, 2045-2074

Wehr, W. (1999): Granulatumhüllte Anker und Nägel -- Sandanker--. Publication of the institute for soil and rock mechanics, Karlsruhe university, vol. 146.

Wehr, W. (1999a): Schottersäulen; Das Verhalten von einzelnen Säulen und Säulengruppen. Geotechnik, Heft 1/1999, S. 40-47

Wehr, W. (2004): Stone columns --- single columns and group behaviour, 5th Int. Conf. On Ground improvement techniques, Malaysia, 329-340

Witt, K.J. (1978): Versagensmechanismus einzeln belasteter Schottersäulen im bindigen Untergrund bei plötzlicher Belastung. Thesis of the institute for soil and rock mechanics, Karlsruhe university

Wood D.M., Hu. W. (1997): Mechanisms of load transfer deduced from failure modes of model stone column foundations. Int. Symposium on Deformation and Progressive Failure in Geomechanics, 5-7.Oct. 1997, Nagoya, Japan, 799-804.